

Flux Motion Studies by Means of Temperature Measurement in Magnetizing Processes for HTSC Bulks

Hiroyuki Fujishiro, Tetsuo Oka, Kazuya Yokoyama, Masahiko Kaneyama, and Koshichi Noto

Abstract—The temperature rises $\Delta T(t)$ of cryo-cooled Sm-BaCuO bulk superconductor have been measured after applying the pulse magnetic field from $B_{\text{ex}} = 3.01$ to 5.42 T for various initial stage temperatures ($T_s = 40$ K \sim 70 K). For each T_s and B_{ex} , the observed systematic change of ΔT and the trapped magnetic field B_T can be explained in terms of the diagram of the maximum temperature measured at the bulk center surface ($T_{0_{\text{max}}}$) vs. B_T . The maximum temperature rise ΔT_{max} decreases with increasing T_s under the identical B_{ex} .

Index Terms—High T_c bulk superconductors, pinning and viscous loss, pulse field magnetizing, temperature measurement.

I. INTRODUCTION

FOR the practical applications of the melt-processed RE-BaCuO superconductors (RE: rare earth ions), the pulse field magnetizing (PFM) have been intensively investigated and developed as well as the static field-cooled magnetizing (FCM) [1]. It is necessary to realize a wider space with higher magnetic field for the applications such as a magnetic separation. For this purpose, new proposals using large-size bulk crystals (e.g., ~ 100 mm ϕ) [2] or the assembly of the several small-size bulks [3] have been made. In case of magnetizing these bulks, it is expensive and is not functional to use a superconducting magnet with a large bore, in which these bulks are to be inserted. The PFM has a promising potential to solve these difficulties because of the relatively compact and inexpensive setup. However, the trapped magnetic field (B_T) in bulks by PFM is currently lower than that by FCM ($B_T(\text{FC})$) below the liquid nitrogen temperature [4]. The main cause has been attributed to the temperature rise ΔT due to the dynamical motion of the magnetic fluxes against the vortex pinning force F_p and the viscous force F_v . However, there have been few systematic experimental studies to relate ΔT with the B_T value. We investigated

the time evolution and spatial distribution of $\Delta T(t)$ on the surface of the cryo-cooled YBaCuO [5] and SmBaCuO [6] bulk superconductors after applying the pulse fields, where the initial stage temperature T_s was maintained in 38 K. It has been found that heat is mainly generated in the peripheral region of the bulk disk and diffuses toward the central region. The magnetic fluxes have been confirmed to move more easily through the growth sector regions (GSR's) than along the growth sector boundaries (GSB's). These results were consistent with the distribution of B_T .

In this paper, we investigate the time and position dependence of $\Delta T(t)$ at various T_s (40 K \sim 70 K) after applying the pulse magnetic field from $B_{\text{ex}} = 3.01$ to 5.42 T for the cryo-cooled SmBaCuO bulk superconductor. Since both F_p and F_v values depend on T_s and B_{ex} , the $\Delta T(t)$ measurements are expected to offer the important clues to enhance B_T .

II. EXPERIMENTAL PROCEDURE

A highly c-axis oriented SmBaCuO bulk superconductor of disk shape with 46 mm in diameter and 15 mm in thickness was fabricated by Dowa Mining Co., Ltd, which consisted of 4 growth sectors (GSR1-GSR4) [6]. The bulk was composed of SmBa₂Cu₃O_y (Sm123) and Sm₂BaCuO₅ (Sm211) with the molar ratio of Sm123 : Sm211 = 1.0 : 0.3, 15.0 wt% Ag₂O powder and 0.5 wt% Pt powder. The bulk was uniformly impregnated by epoxy resin in vacuum and the epoxy resin layer on both upper and bottom sides of the bulk disk was removed in order to measure the precise temperature on the bulk surface and to reduce the thermal contact resistance against the cold stage. Fig. 1 shows the positions of the temperature measurements on the bulk, which was tightly stuck on the cold stage of a Gifford McMahon (GM) cycle helium refrigerator (AISIN, GR103). The initial stage temperature T_s was changed from 40 K to 70 K. The temperatures, T_0 at the center of the bulk (P0) and, $T_1 - T_4$ at P1-P4 in the four GSR's were measured by chromel-constantan thermocouples (76 m in diameter) adhered to the upper bulk surface using GE7031 varnish. P1 \sim P4 were situated on the central lines of each GSR 9 mm apart from P0. Each temperature was measured about 7 times/s just after applying the pulse field.

The bulk crystal was magnetized using a pulse coil dipped in liquid N₂. The rise time of the pulse field B_{ex} was about ~ 10 ms. The strength of B_{ex} was determined from the current flowing through the coil, which ranged from 3.01 T to 5.42 T. The Hall sensor (F.W. Bell, model BHT-921) was adhered to the

Manuscript received October 20, 2003. This work was supported in part by Japan Science and Technology Corporation under the Joint-Research Project for Regional Intensive in the Iwate Prefecture on "Development of practical applications of magnetic field technology for use in the region and in everyday living."

H. Fujishiro and M. Kaneyama are with the Faculty of Engineering, Iwate University, Morioka, 020-8551 Japan (e-mail: fujishiro@iwate-u.ac.jp; t2203004@iwate-u.ac.jp).

T. Oka and K. Yokoyama are with the Iwate Industrial Promotion Center, Morioka 020-0852, Japan (e-mail: toka@iwate-techno.com; yoko@iwate-techno.com).

K. Noto was with the Faculty of Engineering, Iwate University. He is now with Iwate Industrial Promotion Center, Morioka 020-0852, Japan (e-mail: notok@abox2.so-net.ne.jp).

Digital Object Identifier 10.1109/TASC.2004.830392

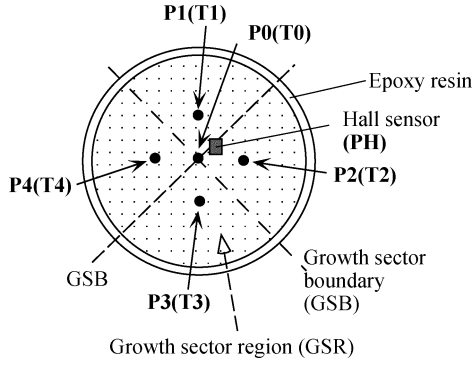


Fig. 1. The positions for the temperature and trapped field measurements on the surface of the SmBaCuO bulk. P0–P4 for the temperature measurement of $T_0 - T_4$ are indicated. The trapped fields $B_T^{3\text{mm}0} - B_T^{3\text{mm}4}$ are also measured at 3 mm just above P0–P4 by a scanning Hall sensor. The trapped field B_T on the bulk surface is measured using a fixed Hall sensor at PH.

position PH, 2.5 mm apart from P0 as shown in Fig. 1, which monitored the B_T value. The two-dimensional distribution of the trapped magnetic field $B_T^{3\text{mm}}$ was monitored using an axial type Hall sensor, which scanned 3 mm above the bulk surface stepwise with a pitch of 1.2 mm. The $B_T^{3\text{mm}}$ values at P0~P4 ($B_T^{3\text{mm}0} \sim B_T^{3\text{mm}4}$) were extracted from the distribution. The trapped field $B_T(\text{FC})$ by FCM was also measured at several temperatures using a cryo-cooled superconducting magnet. During FCM, the static magnetic field of 5 T was decreased down to 0 T in 18 min.

III. RESULTS AND DISCUSSION

Figs. 2(a) and 2(b) show the time evolutions of temperatures $T_0(t) \sim T_4(t)$ for P0~P4 at $T_s = 40$ K after applying the pulse field of 3.01 T and 4.64 T, respectively. Figs. 2(c) and (d) show $T_0(t) \sim T_4(t)$ at $T_s = 50$ K after applying the pulse field of 3.01 T and 4.64 T. The insets of each figure present the $B_T^{3\text{mm}}$ values at P0~P4. It can be seen that the maximum temperature rise ΔT_{max} , the time evolution of temperature, and the $B_T^{3\text{mm}}$ value for each position change depending on the T_s and B_{ex} values. In Fig. 2(a) for $B_{\text{ex}} = 3.01$ T at $T_s = 40$ K, $T_2(t)$ and $T_3(t)$ rise up first with $\Delta T_{\text{max}} \sim 8$ K, followed by $T_4(t)$ and $T_1(t)$, and $T_0(t)$ rise up latest. $T_2(t)$ and $T_3(t)$ show a characteristic peak at $t = 1.8$ s, but the others increase moderately and then reach a maximum at $t = 5 \sim 10$ s ($\Delta T_{\text{max}} \sim 5$ K). All the temperatures return to the initial ones in about 10 minutes. The rapid and large rise of T_2 and T_3 with a characteristic peak means that the powerful heat source is located in the very vicinity of P2 and P3. Since the flux motion necessarily generates heat inside the bulk through the pinning power loss P_p and the viscous flow power loss P_v , such a rapid rise suggests the existence of the easy path for the flux motion due to relatively weaker pinning force F_p of GSR2 and GSR3. In Fig. 2(b), $T_2(t)$, $T_3(t)$ and $T_4(t)$ rise up faster with a clear peak ($\Delta T_{\text{max}} \sim 33$ K), followed by $T_1(t)$, and $T_0(t)$ rise up latest ($\Delta T_{\text{max}} \sim 28$ K). ΔT_{max} increases with increasing B_{ex} and the spatial distribution of the generated heat depends on B_{ex} .

In Fig. 2(c) for $B_{\text{ex}} = 3.01$ T at $T_s = 50$ K, $T_2(t)$, $T_3(t)$ and $T_4(t)$ rise up first with a clear peak at $t = 1.8$ s, followed by $T_1(t)$, and then $T_0(t)$ rise up latest. ΔT_{max} is ~ 8 K for T_2, T_3

and T_4 , which is similar to that for $B_{\text{ex}} = 3.01$ T at $T_s = 40$ K shown in Fig. 2(a). In Fig. 2(d), on the other hand, $T(t)$'s for P1~P4 rise up simultaneously and steeply and do not show a clear peak. ΔT_{max} is ~ 22 K and slightly smaller than those for $B_{\text{ex}} = 4.64$ T at $T_s = 40$ K shown in Fig. 2(b). The rapid rise in $T_1 - T_4$ means that the fluxes penetrate pretty uniformly through the surfaces of the circumference of the 4 GSR's. In all the cases of the flux penetration from $T_s = 40$ K to 70 K, $T_0(t)$ at the center of the bulk rise up latest, because the main heat generation always takes place in the peripheral region where the magnetic fluxes move faster.

The distribution of $B_T^{3\text{mm}}$ also changes depending on T_s and B_{ex} . In the inset of Fig. 2(a) for $B_{\text{ex}} = 3.01$ T at 40 K, $B_T^{3\text{mm}}$ is larger for P2 ($B_T^{3\text{mm}2} = 0.8$ T) and P3 ($B_T^{3\text{mm}3} = 0.7$ T), where ΔT_{max} is also larger. However, $B_T^{3\text{mm}1}$ and $B_T^{3\text{mm}4}$ are quite small and $\Delta T_{\text{max}1}$ and $\Delta T_{\text{max}4}$ are small as well. The behaviors of $B_T^{3\text{mm}}$ and $T_0(t) \sim T_4(t)$ suggest that the surface barrier against the flux penetration has been destroyed in GSR2 and GSR3 for $B_{\text{ex}} = 3.01$ T. On the other hand, the barriers are kept intact in GSR1 and GSR4. In the inset of Fig. 2(b) for $B_{\text{ex}} = 4.64$ T at 40 K, $B_T^{3\text{mm}}$ is the largest for the GSR1 and the smallest for the GSR3 with a V-shaped distribution, making a contrast to $B_{\text{ex}} = 3.01$ T. This result is consistent with the existence of hard path through P1 and the easy path through P3 for the flux motion. In the higher $T_s (= 50$ K), the behaviors of $B_T^{3\text{mm}}$ change. In the inset of Fig. 2(c) for $B_{\text{ex}} = 3.01$ T at 50 K, $B_T^{3\text{mm}2}$ and $B_T^{3\text{mm}3}$ take similar values to those for $B_{\text{ex}} = 3.01$ T at 40 K. However, $B_T^{3\text{mm}4}$ increases from 0.36 T (40 K) to 0.88 T (50 K). This result indicates that the surface barrier against the flux penetration is destroyed at 50 K also in GSR4 and that B_T and ΔT_{max} increase, resultantly. In the inset of Fig. 2(d), the $B_T^{3\text{mm}}$ values decrease at P1, P2, and P4, and the V-shaped $B_T^{3\text{mm}}$ distribution is more broadened compared with those for $B_{\text{ex}} = 4.64$ T at 40 K.

We define the rise time $t(60\%)$ to reach 60% of the maximum temperature rise ΔT_{max} . Figs. 3(a) and 3(b) show $t(60\%)$ as a function of T_s for $B_{\text{ex}} = 3.01$ and 4.64 T. In Fig. 3(a), $t(60\%)$ for T_2 and T_3 is smaller at $T_s = 40$ K because of the destruction of the surface barrier. $t(60\%)$ for T_4 and T_1 become short at $T_s = 50$ K and 60 K, respectively, for the same reason. All the surface barriers in the circumference region against the flux penetration are destroyed at $T_s \geq 60$ K for $B_{\text{ex}} = 3.01$ T. These results are caused by the decrease of F_p with the increase in T_s . The $t(60\%)$ value is determined by the thermal diffusivity $\alpha(T)$ of the bulk and the distance between the measuring point and the heat source. $\alpha(T)$ decreases with increasing T ($\alpha = 23.0$ and 8.2 mm²/s at 40 K and 70 K, respectively) [7]. Accordingly, the decrease of $t(60\%)$ at P4 and P1 with increasing T_s does not come from $\alpha(T)$, but originates from the approach of the heat source to P4 and P1. In Fig. 3(b) for $B_{\text{ex}} = 4.64$ T, $t(60\%)$ for P1~P4 is 0.9~1.2 s and independent of T_s and the position. These results are consistent with the uniform flux intrusion and heat generation. On the other hand, $t(60\%)$ at P0 shows a large value (2.4~3.5 s) and monotonically increases with increasing T_s , which is attributable to the decrease of $\alpha(T)$.

Fig. 4 shows $\Delta T_{0\text{max}}$ at P0 for each T_s as a function of B_{ex} . The inset presents the B_{ex} dependence of B_T monitored by the Hall sensor fixed at PH shown in Fig. 1. (note that P0

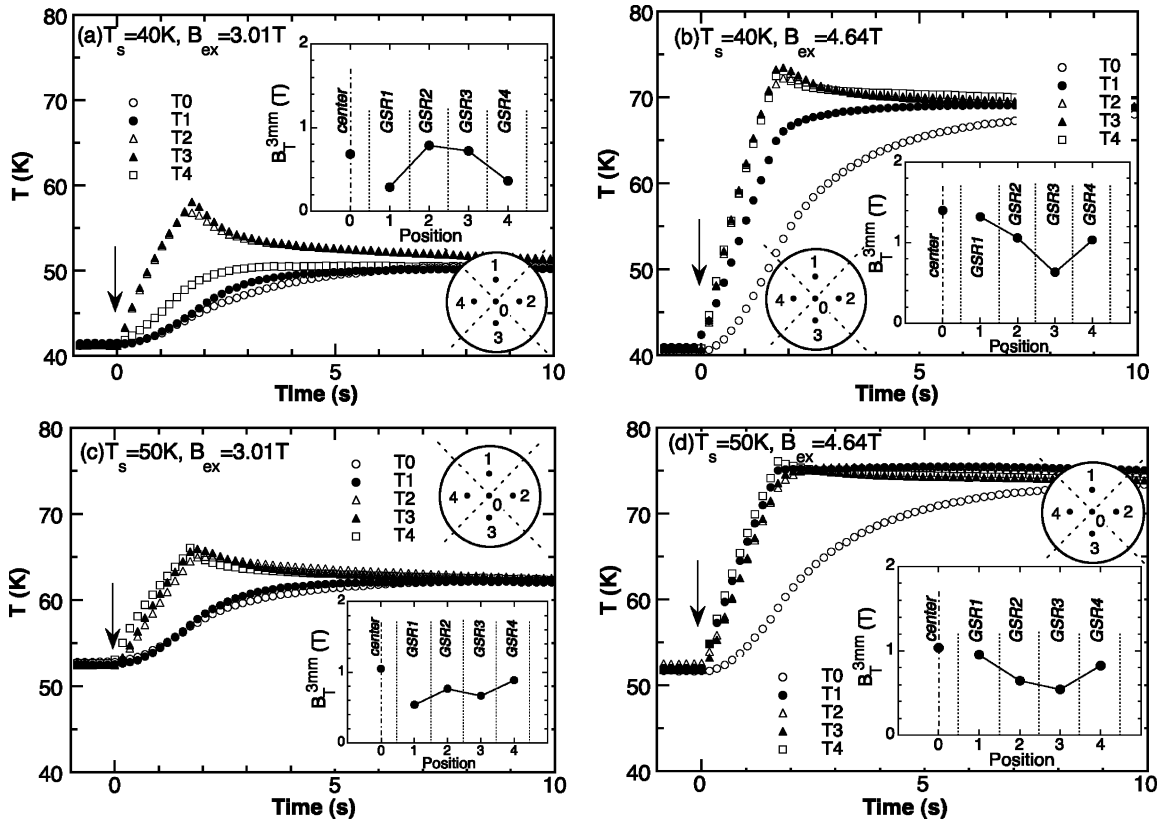


Fig. 2. The time evolution of temperatures $T_0(t) \sim T_4(t)$ for P0~P4 at $T_s = 40$ K after applying the pulse field of (a) 3.01 T and (b) 4.64 T, respectively. (c) and (d) show $T_0(t) \sim T_4(t)$ at $T_s = 50$ K after applying the same pulse fields as (a) and (b), respectively. The insets of figures present the $B_T^{3\text{mm}}$ values at each position.

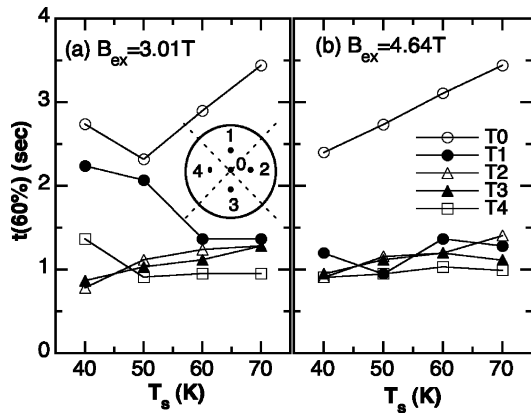


Fig. 3. The $t(60\%)$ value at the positions (P0~P4) as a function of the initial stage temperature T_s for (a) $B_{\text{ex}} = 3.01$ and (b) 4.64 T.

is the nearest position to PH). For each T_s , $\Delta T_{0,\text{max}}$ increases and then shows a saturation tendency with increasing B_{ex} . The $\Delta T_{0,\text{max}}$ values are unexpectedly almost identical for each T_s at $B_{\text{ex}} = 3.01$ T, but increases with decreasing T_s , especially for higher B_{ex} . These results can be explained by the decrease of F_p and by the increase of the specific heat C at higher temperature. In the inset of Fig. 4, at $T_s = 40 \sim 60$ K, B_T increases for $B_{\text{ex}} = 3.87$ T in comparison to $B_{\text{ex}} = 3.01$ T, takes a maximum, and decreases with further increase of B_{ex} . B_T at 3.01 T increases with increasing T_s up to 60 K and then decreases. On the other hand, B_T at 5.42 T monotonically decreases with increasing T_s .

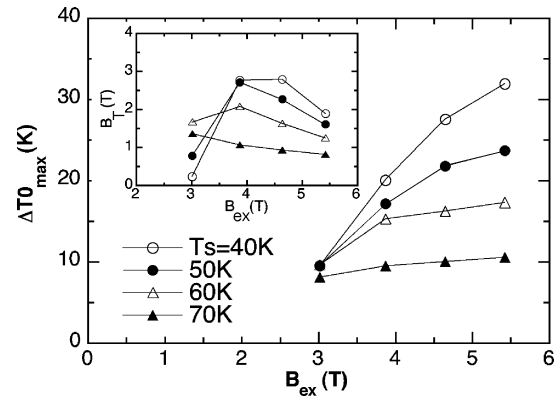


Fig. 4. The maximum temperature rise $\Delta T_{0,\text{max}}$ at P0 for each T_s as a function of B_{ex} . The inset presents the B_{ex} dependence of B_T monitored by the Hall sensor fixed at PH shown in Fig. 1.

Fig. 5 shows the summary of B_T vs. $T_{0,\text{max}}$ in this study. For each T_s , four data sets of $(B_T, T_{0,\text{max}})$ are plotted for $B_{\text{ex}} = 3.01, 3.84, 4.64$ and 5.42 T. The measured trapped field $B_T(\text{FC})$ by FCM corresponding to the temperature $T_{0,\text{max}}$ is also presented. In the case of $T_s = 40$ K, the two data sets of $(B_T, T_{0,\text{max}})$ are situated below the $B_T(\text{FC}) - T_{0,\text{max}}$ line for $B_{\text{ex}} \leq 3.82$ T. For $B_{\text{ex}} \geq 4.64$ T, $T_{0,\text{max}}$ touches the line owing to the large temperature rise and then B_T decreases following the line. In the case of $T_s = 50$ K, only the data set for $B_{\text{ex}} = 3.01$ T is situated below the $B_T(\text{FC}) - T_{0,\text{max}}$ line, and for $B_{\text{ex}} \geq 4.64$ T, $T_{0,\text{max}}$ touches the line and the B_T decreases. On the other hand, for $T_s = 60$ and 70 K, all the data sets touch the line already at

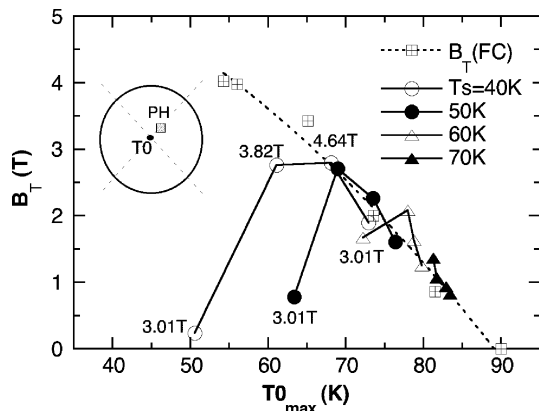


Fig. 5. The summary of the trapped field B_T at PH vs. the maximum temperature $T0_{\max}$ at P0. For each T_s , four data sets of $(B_T, T0_{\max})$ are plotted for $B_{\text{ex}} = 3.01, 3.84, 4.64$ and 5.42 T. The trapped field $B_T(\text{FC})$ by FCM is also shown.

$B_{\text{ex}} = 3.01$ T and B_T monotonically decreases with increasing B_{ex} . These results demonstrate that the flux trapping ability by the PFM technique can be systematically explained as limited by the $B_T(\text{FC}) - T0_{\max}$ line [6].

In summary, we measured the temperature rises $\Delta T(t)$ of a cryo-cooled SmBaCuO bulk superconductor after applying the pulse magnetic fields (~ 10 ms of the rise time) from $B_{\text{ex}} = 3.01$ to 5.42 T for various initial stage temperatures ($T_s = 40 \sim 70$ K). The maximum temperature rise ΔT_{\max} , the time evolution of temperature $T0(t) \sim T4(t)$, and the trapped field B_T^3 mm value for each position changes depending on the T_s and B_{ex} values. When T_s increases, ΔT_{\max} decreases due to the reduction of the pinning force F_p and the specific heat as shown in Fig. 4. As a result, the magnetic fluxes easily penetrate into the bulk and can be trapped at higher T_s even for relatively lower B_{ex} value; B_T increases with increasing T_s for $B_{\text{ex}} = 3.01$ T, as shown in the inset of Fig. 4. However, at higher T_s , there is only small temperature margin between T_s and the superconducting transition temperature $T_c (= 93$ K) and the flux trapping

ability of the bulk necessarily decreases. In this sense, T_s must be decreased as low as possible in order to obtain the higher B_T values. The B_T behavior at the various T_s and for various B_{ex} can be clearly understood on the basis of the $B_T(\text{FC}) - T0_{\max}$ line, which corresponds to the maximum-trapped field of the bulk.

The temperature rise ΔT is caused by both the pinning power loss P_p and the viscous flow power loss P_v . Which power loss is dominant for ΔT in the case of each T_s and B_{ex} is open to question. In order to clarify this problem and to improve the PFM technique for the B_T enhancement, it is necessary to analyze the data more closely based on the generated heat Q for various T_s and B_{ex} .

ACKNOWLEDGMENT

The authors greatly thank Prof. M. Ikebe of Iwate University for valuable suggestions.

REFERENCES

- [1] U. Mizutani, T. Oka, Y. Itoh, Y. Yanagi, M. Yoshikawa, and H. Ikuta, "Pulse-field magnetization applied to high- T_c superconductors," *IEEE Trans. Appl. Supercond.*, vol. 6, pp. 235–246, 1998.
- [2] T. Fujimoto, M. Morita, N. Masahashi, and T. Kaneko, "Fabrication of 100 mm-diameter Y-Ba-Cu-O bulk QMG superconductors with large levitation forces," in *Inst. Phys. Conf. Ser.*, vol. 167, 2000, pp. 79–83.
- [3] T. Oka, K. Yokoyama, and K. Noto, "Construction of a strong magnetic field generator with wide magnetic poles by bulk superconductors," *Physica C*.
- [4] H. Ishihara, H. Ikuta, Y. Itoh, Y. Yanagi, M. Yoshikawa, T. Oka, and U. Mizutani, "Pulsed field magnetization of melt-processed Sm-Ba-Cu-O," *Physica C*, vol. 357–360, pp. 763–766, 2001.
- [5] H. Fujishiro, T. Oka, K. Yokoyama, and K. Noto, "Time evolution and spatial distribution of temperature in YBCO bulk superconductor after pulse field magnetizing," *Supercond. Sci. Tech.*, vol. 16, pp. 809–814, 2003.
- [6] —, "Temperature rise in Sm-based bulk superconductor after applying iterative pulse fields," *Supercond. Sci. Tech.*, vol. 17, pp. 51–57, 2004.
- [7] H. Fujishiro and S. Kohayashi, "Thermal conductivity, thermal diffusivity and thermoelectric power in Sm-based bulk superconductors," *IEEE Trans. Appl. Supercond.*, vol. 12, no. 1, pp. 1124–1127, March 2002.